ELECTRO-KINETICALLY MODULATED PERISTALTIC MECHANISM OF JEFFREY LIQUID THROUGH A MICRO-CHANNEL WITH VARIABLE VISCOSITY

by

Rajashekhar CHOUDHARI[a], Hanumesh VAIDYA[b], Fateh MEBAREK-OUDINA[c], Abderrahim WAKIF[d], Manjunatha GUDEKOTE[e,*], Kerehalli Vinayaka PRASAD[b], Kuppalapalle VAJRAVELU[f], and Shivaraya KERIYAPA[b]

[a] Department of Mathematics, Karnataka State Akkamahadevi Women's University, Vijayapura, Karnataka, India
[b] Department of Mathematics, Vijayanagara Sri Krishnadevaraya University, Ballari, Karnataka, India
[c] Department of Physics, Faculty of Sciences, University of 20 août 1955-Skikda, Skikda, Algeria
[d] Laboratory of Mechanics, Faculty of Sciences Ain Chock, Hassan II University, Casablanca, Morocco
[e] Department of Mathematics, Manipal Institute of Technology, Manipal Academy of Higher Education, Manipal, Karnataka, India
[f] Department of Mathematics, University of Central Florida, Orlando, Fla., USA,

Original scientific paper
https://doi.org/10.2298/TSCI21S2271C

A theoretical model is developed to stimulate electro-kinetic transfer through peristaltic movement in a micro-channel. The effect of variable viscosity and wall properties are considered. The long wavelength and small Reynolds number approximations are supposed to simplify the governing formulas. Debye-Huckel linearization is also utilized. The perturbation technique is utilized to solve the governing non-linear equations. The graphical outcomes are presented for velocity and streamlines.

Key words: *debye length, peristalsis, electroosmosis, variable viscosity, heat and mass transport, wall properties*

Introduction

Peristalsis is a vital liquid physiological transportation mechanism in living organs. It is caused by the constant tightening and relaxation of the vessel walls. The intestinal network, lymphatic vessels, glandular ducts, and blood vessels are all said to have peristaltic pumping as a built-in property in some cases. Peristalsis-based explorations in the industry include finger and roller pumps, sanitary, and the transportation of several corroding materials. It is used in MRI, endoscopes, heart-lung devices, catheters, and various other bioscience applications. After Latham [1] introduced his work on peristaltic flow, scientists and researchers used experimental, numerical, and analytical techniques to add to the literature under various assumptions and boundary conditions. In this way, some appropriate studies have been reported in [2-5].

* Corresponding author, e-mail: manjunatha.g@manipal.edu

Increasing the rate of liquid circulation to the maximum possible restriction by preparing for appropriate groupings of circulation actuating systems is one of the most significant challenges in the design of microfluidic transportation systems in many of the mentioned appliances. Because it does not require the standard relocating components attributed to traditional micro-pumps, it has significant advantages in microfluidic pumping. On the other hand, electro-osmosis has proven to be a more straightforward mechanism for creating nearly plug-shaped velocity profiles in micro-channels by manipulating the communication of an applied axial electrical field with local fee density gradients near the liquid-solid user interface. Driven by the application of electroosmotic transport on the peristaltic device, Chakraborty [6] designed the peristaltic circulation by taking an electric field. Non-etheless, a slim electrical double layer (EDL) estimation was carried. Bandopadhyay *et al.* [7] modified another model to review the stress circulation, channel size, and impacts of the electric field and EDL thickness. any theoretical, as well as computational researches on electroosmotic flow with and also without heat transport have been presented [8, 9].

Numerous studies conducted by considering animal physiology found that the biological liquids show variation in viscosity. The consideration is evident because the average animal or human of comparable dimensions consumes as much as two liters of water, causing a modification in the focus of physical fluids over time. Thus, considering the variation in viscosity is an essential factor while examining the peristaltic system. The studies accounting for these properties have assisted in a better understanding of non-Newtonian fluids. Some vital researches regarding the use of the non-Newtonian fluids in modeling and evaluation of peristaltic circulation with variable fluid properties can be found in [10-12]. The current study is the first of its kind in modeling the electro-kinetically modulated peristaltic circulation of Jeffrey liquid with variable viscosity. In addition, the effect of wall properties is considered. The governing equations are simplified through utilizing trusted estimation, namely lubrication, as well as Debye-Huckel estimate. After that, the perturbation strategy solves the resulting equation, and outcomes are contrasted numerically utilizing the MATLAB software program. The impact of relevant parameters on velocity and streamlines are discussed graphically.

Modeling

Flow analysis

The 2-D electrokinetically modulated flow of Jeffrey liquid through a uniform microfluidic channel having width $2\bar{a}$ has been analyzed. The propagation of sinusoidal wave forms this flow at a continuous speed, *c*, along the complaint channel walls. Let $\bar{Y} = \pm\bar{h}(\bar{X}, \bar{t})$ be the lower and upper wall, respectively. Here, propagation of wave is along the axial direction (*x*-axis).

The micro-channel wall equation is given by [8]:

$$\bar{Y} = \pm\bar{h}(\bar{X}, \bar{t}) \pm \left\{ \bar{a} + \bar{b}\sin\left[2\pi \frac{(\bar{X} - c\bar{t})}{\lambda} \right] \right\} \tag{1}$$

Formulations

The governing equation in the laboratory frame of reference for the circulation of Jeffrey liquid in electro-hydrodynamic are [8]:

$$\frac{\partial \bar{U}}{\partial \bar{X}} + \frac{\partial \bar{V}}{\partial \bar{Y}} = 0 \tag{2}$$

$$\rho\left(\frac{\partial \bar{U}}{\partial \bar{t}} + \bar{U}\frac{\partial \bar{U}}{\partial \bar{X}} + \bar{V}\frac{\partial \bar{V}}{\partial \bar{Y}}\right) = -\frac{\partial \bar{P}}{\partial \bar{X}} + \frac{\partial}{\partial \bar{X}}\bar{S}_{\bar{X}\bar{X}} + \frac{\partial}{\partial \bar{Y}}\bar{S}_{\bar{X}\bar{Y}} + \rho_e E_x \tag{3}$$

$$\rho\left(\frac{\partial \bar{U}}{\partial \bar{t}} + \bar{U}\frac{\partial \bar{V}}{\partial \bar{X}} + \bar{V}\frac{\partial \bar{V}}{\partial \bar{Y}}\right) = -\frac{\partial \bar{P}}{\partial \bar{Y}} + \frac{\partial}{\partial \bar{X}}\bar{S}_{\bar{Y}\bar{X}} + \frac{\partial}{\partial \bar{Y}}\bar{S}_{\bar{Y}\bar{Y}} \tag{4}$$

The constitutive equation for Jeffrey liquid is given through [2]:

$$\bar{\tau} = -\bar{p}\bar{I} + \bar{S}, \quad \bar{S} = \frac{\mu(y)}{1+\lambda_1}\left(\dot{\bar{\gamma}} + \lambda_2 \ddot{\bar{\gamma}}\right) \tag{5}$$

where $\bar{\tau}$ is the Cauchy stress tensor, I – the identity tensor, λ_2 – the retardation time, S – the extra stress tensor, λ_1 – the ratio of relaxation to retardation times, $\bar{p}$ – the pressure, and $\dot{\gamma}$ – the shear rate and dots on the quantities specify differentiation through respect to time.

The expression for ϕ is given by [8]:

$$\phi(y) = \frac{\cosh(m_e y)}{\cosh(m_e h)} \tag{6}$$

Non-dimensionalization

The conversion from laboratory frame $(\bar{X}, \bar{Y})$ to wave frame of references $(\bar{x}, \bar{y})$ is:

$$\bar{y} = \bar{Y}, \quad x = \bar{X} - c\bar{t}, \quad \bar{p}(\bar{x}, \bar{y}) = \bar{P}(\bar{X}, \bar{Y}, \bar{t}), \quad \bar{u}(\bar{x}, \bar{y}) = \bar{U}(\bar{X}, \bar{Y}, \bar{t}) - c$$

$$\bar{v}(\bar{x}, \bar{y}) = \bar{V}(\bar{X}, \bar{Y}, \bar{t}) \tag{7}$$

The previous conversions are utilized in eqs. (2)-(4) and then introducing the dimensionless variables:

$$x = \frac{2\pi\bar{x}}{\lambda}, \quad y = \frac{\bar{y}}{a}, \quad t = \frac{2\pi c\bar{t}}{\lambda}, \quad u = \frac{\bar{u}}{c}, \quad v = \frac{\bar{v}}{c}, \quad p = \frac{2\pi a^2 \bar{p}}{\lambda \mu_0 c}, \quad \alpha_1 = \frac{2\pi a}{\lambda}$$

$$h = \frac{\bar{h}}{a}, \quad m_{\mathrm{e}} = \frac{a}{\lambda_{\mathrm{D}}}, \quad n = \frac{\bar{n}}{n_0}, \quad \epsilon = \frac{b}{a}, \quad \theta = \frac{\bar{T} - T_0}{T_0}, \quad \sigma = \frac{\bar{C} - C_0}{C_0}, \quad \lambda_D = \frac{1}{eZ_v}\sqrt{\frac{T_0 \xi K_B}{2n_0}}$$

$$\phi = \frac{ez_v\bar{\phi}}{T_{av}K_B}, \quad U_{\mathrm{hs}} = -\frac{E_x \xi}{c\mu_0}, \quad S = \frac{a\bar{S}}{c\mu_0}, \quad \psi = \frac{\bar{\psi}}{ca}, \quad u = \frac{\partial \psi}{\partial y}, \quad v = -\alpha_1 \frac{\partial \psi}{\partial x}, \quad \mathrm{Re} = \frac{\rho c a}{\mu_0}$$

$$\mu_0 = \frac{\overline{\mu_0}}{\mu}, \quad E_1 = \frac{\tau a^3}{\mu_0 \lambda^3 c}, \quad E_2 = \frac{n_1 a^3 c}{\mu_0 \lambda^3 c}, \quad E_3 = \frac{n_2 a^3}{\mu_0 \lambda^3} \tag{8}$$

where λ_{D} is the Debye length, y – the dimensionless transverse coordinate, U_{hs} – the Helmholtz–Smoluchowski velocity, m_{e} – the electroosmotic term, p – the dimensionless pressure, α_1 – the peristaltic wave number, ψ – a dimensionless stream function, S – the non-dimensional shear stress, Re – the Reynolds number, ϵ – the amplitude ratio, and x – the dimensionless axial coordinate.

The governing equation of motion of the flexible wall may be expressed [3]:

$$R(h) = p - p_0 \tag{9}$$

where R is an operator, which is used to represent the motion of stretched membrane with viscous damping forces such that:

$$R = -\tau \frac{\partial^2}{\partial x^2} + n_1 \frac{\partial^2}{\partial t^2} + n_2 \frac{\partial}{\partial t} \tag{10}$$

Continuity of stress at $y = h$ and using x-momentum equation yields:

$$\frac{\partial R(h)}{\partial x} = \frac{\partial p}{\partial x} = \frac{\partial}{\partial y} S_{xy} + \rho_e E_x \tag{11}$$

where τ is the elastic tension in the membrane, n_1 – the mass per unit area, n_2 – the coefficient of viscous damping forces, p_0 – the pressure on the outside surface of the wall due to the tension in the muscles, and h – the dimensional slip parameter. We assumed $p_0 = 0$.

Equation (2) is identically satisfied and, from eqs. (3)-(6), subject to long-wavelength assumption and ignoring superior powers of α_1, we acquire:

$$\frac{\partial p}{\partial x} = \frac{\partial}{\partial y}\left[\left(\frac{1-\alpha y}{1+\lambda_1}\right)\frac{\partial^2 \psi}{\partial y^2}\right] + m_e^2 U_{hs}\phi \tag{12}$$

$$\frac{\partial p}{\partial y} = 0 \tag{13}$$

The non-dimensional boundary conditions are:

$$\frac{\partial^2 \psi}{\partial y^2} = 0, \quad \psi = 0, \quad \text{at} \quad y = 0 \tag{14}$$

$$\frac{\partial \psi}{\partial y} = -1, \quad \text{at} \quad y = h(x) = 1 + \epsilon \sin x \tag{15}$$

The expression for variable viscosity is:

$$\mu(y) = 1 - \alpha y \quad \text{for} \quad \alpha \ll 1 \tag{16}$$

here α is the coefficient of viscosity.

Perturbation solution

Equations (12) and (13) specify a governing differential system with boundary conditions (14) and (15) that are extremely non-linear. It is impossible to find an exact solution to this system of equations. As a result, the system can be solved analytically using the perturbation method, which uses variable viscosity, α, as perturbation term. The solution of 0^{th} and 1^{st} order systems along with boundary conditions are obtained using the MATLAB2019b programming. The separate code has been written to acquire the solutions for velocity and streamline.

Outcome and discussion

Velocity profiles

Figure 1 depicts the effect of relevant parameters on velocity. The velocity profiles have a parabolic shape due to an optimum velocity in the conduit's center. Figure 1(a) shows that as U_{hs}, or the optimal electroosmotic velocity (or Helmholtz-Smoluchowski velocity), increases from –1 to 4, the axial circulation has substantial momentum. For larger U_{hs}, a subsequent boost in an axial electric field causes a significant deceleration. The circulation is supported and obstructed by an essential electrical field strength. The more critical values of m_e in fig. 1(b) initially reduce the velocity profiles. Furthermore, there is a slight variation in velocity profiles for higher values. The mutual of Debye length is the Debye-Huckel specification. Because increased ion migration occurs as we move away from the indicted area, decreasing Debye length, *i.e.*, rising Debye-Huckel term, is thought to increase electrical capacity. As a result,

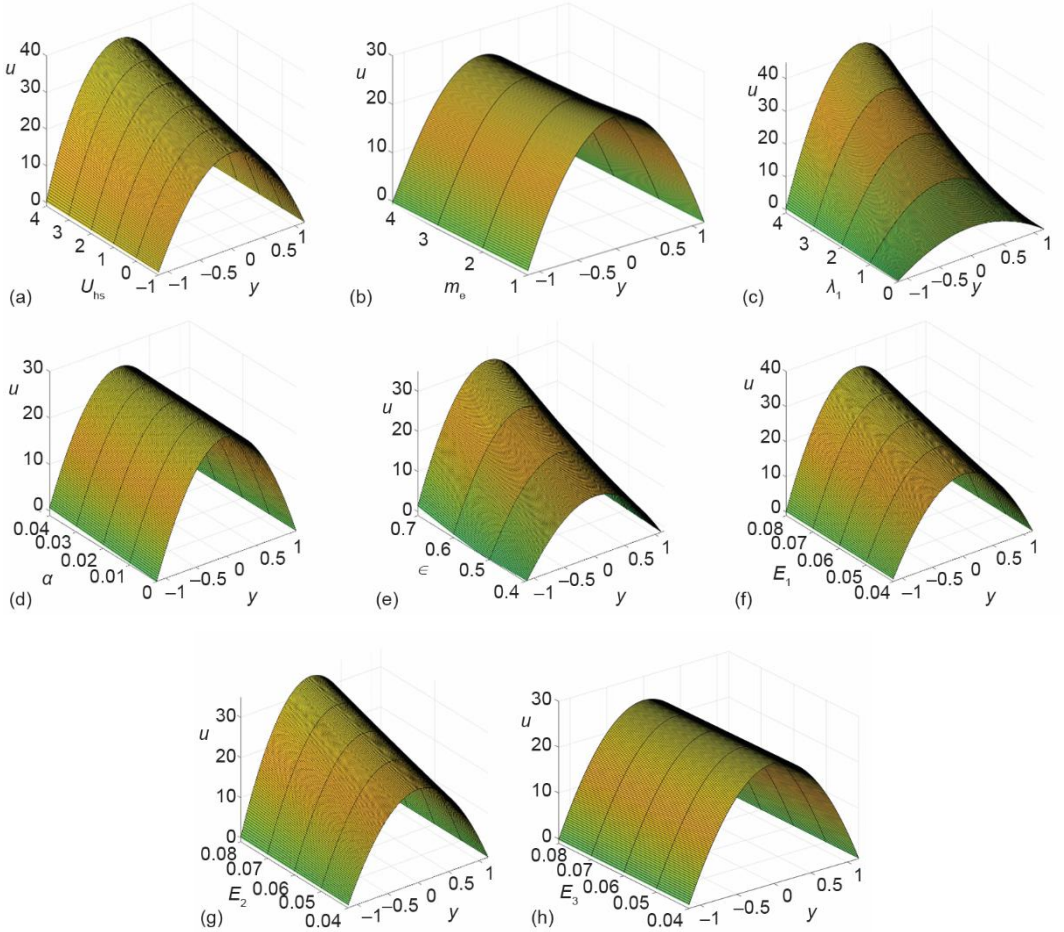

Figure 1. The $u(y)$ for varying (a) U_{hs}, (b) m_e, (c) λ_1, (d) α, (e) ϵ, (f) E_1, (g) E_2, and (h) E_3

Debye length is a vital style criterion in managing potential electrical variation, which significantly impacts the axial velocity field. Figure 1(c) has been drawn for multiple values of the Jeffrey parameter. The velocity profile improves as the Jeffrey criterion rises, as shown in this graph. It is worth noting that by taking $\lambda_1 = 0$, the outcome decreases to Newtonian liquid. Figure 1(d) depicts the effect of variable viscosity on velocity profiles. The velocity profile enhances for more significant values of variable viscosity. Because a boost in variable viscosity parameters decreases the fluid's viscosity and thus improves the fluid circulation. Figure 1(e) reveals a rise in the velocity profiles for more significant values of amplitude ratio. Amplitude ratio is the relation between wave amplitude to channel width. Hence, a boost in amplitude ratio significantly improves the velocity profiles. The impact of flexibility, mass parameter, and viscous damping force term is exposed in figs. 1(f)-1(h). With an improvement in the flexibility parameter, the fluid viscosity weakens since the particle moves at higher speeds. As the mass per unit area, the liquid travel particles freely develop the speed uplift. Since damping operates to resist the circulation speed because of energy loss, a minimizing response is apprehended. Clinically, when blood walls are flexible or the mass per unit surface rises (like in blood capillaries), the exchange of oxygen, water, and other nutrients becomes simple. The damping tends to react oppositely.

Trapping phenomenon

It is usually known that the phenomenon of trapping is an integral element of peristaltic research studies. The liquid, therefore, caught within the bolus is pushed forward along through the peristaltic wave. Figure 2 shows a streamlined makeup for various U_{hs}. It shows that the build-up of streamlines reduces through a rise in U_{hs}. Hence, stronger U_{hs} means a more powerful external electrical field. The variety of enclosed boluses considerably diminishes for large values of U_{hs}. Figure 3 shows that the combination of enclosed boluses increases with a rise in the electroosmotic criterion. For greater m_e, the enclosed bolus appears stronger in EDL.

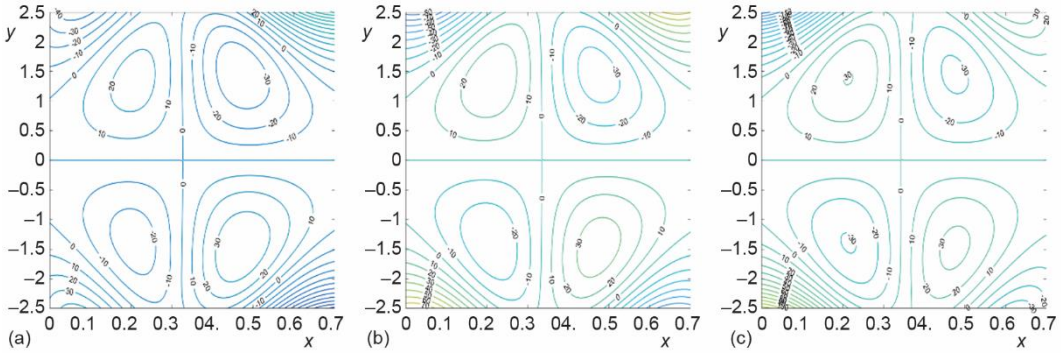

Figure 2. The $\psi(x, y)$ for varying (a) $U_{hs} = -1$, (b) $U_{hs} = 0$, and (c) $U_{hs} = 1$

Conclusions

The influences of electroosmotic, wall properties, and variable viscosity over the peristaltic flow of Jeffrey liquid through a uniform channel are analyzed. MATLAB2020a programming is utilized to discusses the impact of critical terms over velocity and streamlines. The findings seen in this paper have potential implications in both industry and medical research.

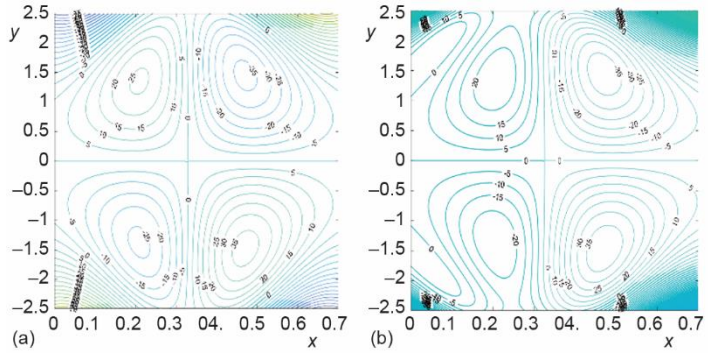

Figure 3. The $\psi(x, y)$ for varying (a) $m_e = 1$ and (b) $m_e = 3$

The present work provides a fair theoretical approximation for further research in this direction. The main findings of the model are summarized as follows.

- The velocity profiles rise for higher values of optimum electroosmotic velocity.
- The electroosmotic specification is a reducing function of velocity.
- The Jeffrey criterion boosts the velocity profiles.
- The variable viscosity boosts the velocity profiles.
- The accumulation of streamlines reduces with a boost in maximum electroosmotic velocity.
- The number of enclosed boluses augments through a boost in the electroosmotic criterion.

References

[1] Latham, T. W., *Fluid Motions in a Peristaltic Pump*, M. Sc. thesis, MIT Boston, Mass., USA, 1966
[2] Kothandapani, M., Srinivas, S., Peristaltic Transport of a Jeffrey Fluid Under the Effect of Magnetic Field in an Asymmetric Channel, *Int. J. Non. Linear. Mech., 43* (2008), 9, pp. 915-924
[3] Srinivas, S., *et al.*, The Influence of Slip Conditions, Wall Properties and Heat Transfer on MHD Peristaltic Transport, *Comput. Phys. Commun., 180* (2009), 11, pp. 2115-2122
[4] Vaidya, H., *et al*., Role of Slip and Heat Transfer on Peristaltic Transport of Herschel-Bulkley Fluid Through an Elastic Tube, *Multidiscip. Model. Mater. Struct., 14* (2018), 5, pp. 940-959
[5] Abbas, Z., *et al*., Peristaltic Transport of a Casson Fluid in a Non-Uniform Inclined Tube with Rosseland Approximation and Wall Properties, *Arab. J. Sci. Eng., 46* (2021), pp. 1997-2007
[6] Chakraborty, S., Augmentation of Peristaltic Microflows Through Electro-Osmotic Mechanisms, *J. Phys. D. Appl. Phys., 39* (2006), 24, pp. 5356-5363
[7] Bandopadhyay, A., *et al*., Electroosmosis-Modulated Peristaltic Transport in Microfluidic Channels, *Phys. Fluids, 28* (2016), 5, 052002-23
[8] Waheed, S., *et al*., Study of Heat and Mass Transfer in Electroosmotic Flow of Third Order Fluid through Peristaltic Microchannels, *Appl. Sci., 9* (2019), 10, ID 2164
[9] Waheed, S., *et al*., Electrothermal Transport of Third-Order Fluids Regulated by Peristaltic Pumping, *J. Biol. Phys., 46* (2020), Feb., pp. 45-65
[10] Vaidya, H., *et al*., Effect of Variable Liquid Properties on Peristaltic Flow of a Rabinowitsch Fluid in an Inclined Convective Porous Channel, *Eur. Phys. J. Plus*, 134 (2019), 5, ID 231
[11] Chu, Y. M., *et al.*, Entropy Analysis in the Rabinowitsch Fluid Model Through Inclined Wavy Channel: Constant and Variable Properties, *Int. Commun. Heat Mass Transf., 119* (2020), ID 104980
[12] Vaidya, H., *et al.*, Channel Flow of MHD Bingham Fluid Due to PERISTALSis with Multiple Chemical Reactions: An Application to Blood Flow Through Narrow Arteries, *SN Appl. Sci., 3* (2021), ID 186

Paper submitted: April 23, 2021
Paper revised: May 5, 2021
Paper accepted: May 7, 2021